UNCLASSIFIED

SECURITY CLASSIFICATION OF THIS PAGE *(When Data Entered)*

REPORT DOCUMENTATION PAGE		READ INSTRUCTIONS BEFORE COMPLETING FORM
1. REPORT NUMBER	2. GOVT ACCESSION NO.	3. RECIPIENT'S CATALOG NUMBER
4. TITLE *(and Subtitle)* IMPULSE STIMULATED CRYSTALLIZATION IN AMORPHOUS SEMICONDUCTING FILMS		5. TYPE OF REPORT & PERIOD COVERED Technical Report 6. PERFORMING ORG. REPORT NUMBER R-844; UILU-ENG 78-2237
7. AUTHOR(s) C. E. WICKERSHAM G. BAJOR J. E. GREENE		8. CONTRACT OR GRANT NUMBER(s) DAAB-07-72-C-0259
9. PERFORMING ORGANIZATION NAME AND ADDRESS Coordinated Science Laboratory University of Illinois at Urbana-Champaign Urbana, Illinois 61801		10. PROGRAM ELEMENT, PROJECT, TASK AREA & WORK UNIT NUMBERS
11. CONTROLLING OFFICE NAME AND ADDRESS Joint Services Electronics Program		12. REPORT DATE May, 1979 13. NUMBER OF PAGES 36
14. MONITORING AGENCY NAME & ADDRESS*(if different from Controlling Office)*		15. SECURITY CLASS. *(of this report)* UNCLASSIFIED 15a. DECLASSIFICATION/DOWNGRADING SCHEDULE

16. DISTRIBUTION STATEMENT *(of this Report)*

Approved for public release; distribution unlimited

17. DISTRIBUTION STATEMENT *(of the abstract entered in Block 20, if different from Report)*

18. SUPPLEMENTARY NOTES

19. KEY WORDS *(Continue on reverse side if necessary and identify by block number)*

Thin Films
Crystallization
Semiconductors
(InGa)Sb
Optical Memories
Sputtering

20. ABSTRACT *(Continue on reverse side if necessary and identify by block number)*

Rapid irreversible exothermic amorphous-to-polycrystalline phase transitions have recently been reported in amorphous Ge and $In_{1-x}Ga_xSb$ films. Such transformations occur in $\sim 10^{-6}$ sec in a local domain (with a typical diameter of 1 μm) of the film in response to an energy impulse supplied, for example, optically by a pulsed laser or mechanically by a needle tipped stylus. The crystallization front can propagate throughout the film in a cascade process with velocities on the order of several hundred cm/sec if the energy released

DD FORM 1 JAN 73 1473 EDITION OF 1 NOV 65 IS OBSOLETE

UNCLASSIFIED

SECURITY CLASSIFICATION OF THIS PAGE *(When Data Entered)*

20. ABSTRACT (continued)

from the crystallization of one domain is sufficient to trigger the adjacent domain under the existing experimental conditions. Experimental results are presented which demonstrate that propagation of the crystalline front depends upon the sample temperature as well as its thermal history. A simple thermal transport model is also presented which expresses in functional form the parametric requirements for the propagation of impulse stimulated crystallization (ISC). All reported experimental results including the sample temperature and thermal history dependence, variations in the transformed surface topographical structure, and the critical thickness effect can be explained by this model.

UILU-ENG 78-2237

IMPULSE STIMULATED CRYSTALLIZATION IN AMORPHOUS SEMICONDUCTING FILMS

by

C. E. Wickersham, G. Bajor, J. E. Greene

This work was supported in part by the Joint Services Electronics Program (U.S. Army, U.S. Navy and U.S. Air Force) under Contract DAAB-07-72-C-0259.

Impulse Stimulated Crystallization in Amorphous Semiconducting Films

C. E. Wickersham,[†] G. Bajor,[*] and J. E. Greene

Departments of Metallurgy, Mechanical Engineering,
and the Coordinated Science Laboratory
University of Illinois, Urbana 61801

ABSTRACT

Rapid irreversible exothermic amorphous-to-polycrystalline phase transitions have recently been reported in amorphous Ge and $In_{1-x}Ga_xSb$ films. Such transformations occur in ~ 10^{-6} sec in a local domain (with a typical diameter of 1 μm) of the film in response to an energy impulse supplied, for example, optically by a pulsed laser or mechanically by a needle tipped stylus. The crystallization front can propagate throughout the film in a cascade process with velocities on the order of several hundred cm/sec if the energy released from the crystallization of one domain is sufficient to trigger the adjacent domain under the existing experimental conditions. Experimental results are presented which demonstrate that propagation of the crystalline front depends upon the sample temperature as well as its thermal history. A simple thermal transport model is also presented which expresses in functional form the parametric requirements for the propagation of impulse stimulated crystallization (ISC). All reported experimental results including the sample temperature and thermal history dependence, variations in the transformed surface topographical structure, and the critical thickness effect can be explained by this model.

[†]Permanent address: Batelle Columbus Laboratory, Columbus, Ohio.

[*]Permanent address: Technical University of Budapest, Budapest, Hungary.

I. Introduction

Rapid amorphous to crystalline phase transitions have been of interest for use in switching, memory, and other types of electronic devices for many years.[1,2] Most of the work in this area has been centered on inorganic glassy semiconductors such as chalcogenides in which the amorphous state can be obtained using relatively modest quench rates, reportedly as low as several degrees per min.[3] In such materials, reversible switching devices can be fabricated utilizing the formation of conducting filaments through the more highly resistive amorphous semiconductor. The filaments are metallic crystallites formed by electrical joule heating or laser pulses. Such filaments can be "erased" by imposing higher intensity thermal pulses followed by rapid quenching.

Rapid irreversible amorphous-to-crystalline phase transformations which can be made to propagate throughout the bulk of the sample have also been reported in pure amorphous Sb,[4,5] Ge,[6-11] C,[12] and (In,Ga)Sb[13] films. In the case of the Ge and (In,Ga)Sb films, the only materials for which detailed investigations have been carried out, the transformation was triggered by a localized mechanical or optical energy impulse which produced crystallization only in the affected region. If the sum of the energy supplied by external heating and the heat of crystallization released from the transformed domain was sufficient to trigger an adjacent domain, then crystallization propagated throughout the film in a cascade process. A review of reported results in the explosive impulse stimulated crystallization (ISC) of films reveals the following basic features of the transfromation: (1) ISC requires a localized energy impulse for initiation, (2) the transformation is rapid ($t < 1$ msec for a sample with a surface area of 1x1 cm, (3) the transformation is exothermic, (4) the transition

can be suppressed by sample cooling, (5) the transition can be suppressed in favor of normal crystallization by high temperature annealing, (6) the transformed sample exhibits changes in surface topography, (7) the topographical features of a transformed film indicate that the transformation propagates radially outward from the initial impulse or triggering point, and (8) propagation of the transformation cannot be initiated in films thinner than a critical value and the transformation is halted at a critical thickness in films with a thickness gradient.

Figures 1 and 2, taken from reference 13, illustrate many of these features. In Figure 1 the sample resistance is shown as a function of temperature for sputter deposited amorphous GaSb films heated at a rate of 27°C/min. The as-deposited film in curve A was ISC-transformed at ~ 90°C, while the minimum ambient temperature at which the transformation could be induced, T^*, was increased to ~ 175°C for sample B which had been previously annealed at 180°C for 90 min. Sample C was heated up to 270°C without impulsing it, allowing the film to begin crystallization by normal nucleation and grain growth. Following this thermal cycle, ISC could not be initiated at any temperature. The hysteresis effect observed in ISC transformed samples A and Bupon cooling is due to the highly exothermic nature of the transformation. Figure 2 shows the increase in T^* as a function of annealing time at 135°C and 175°C for amorphous $In_{0.4}Ga_{0.6}Sb$ films.

Aymerich and Delunas,[5] Takamori et al.,[6] Kikuchi,[11] and Wickersham et al.[13] have all proposed qualitative energy cascade models of ISC in which the heat generated by the rapid crystallization of a localized domain in the sample triggers the crystallization of an adjacent domain. However these models, by themselves, do not explain several observed features of ISC, for example: the effects os sample thermal history, the suppression of the transition by covering

the surface of the sample with another film,[13] and the fact that ISC does not occur in films thinner than a certain critical value.[6,13]

In the present paper, we present some new experimental results on ISC in amorphous (In,Ga)Sb alloys as well as a single thermal transport model with which all of the above discussed general features of ISC propagation can be explained.

II. Experimental Procedure

(In,Ga)Sb films were grown by multi-target sputter (MTS) deposition on Corning 7059 glass substrates which exhibit a good thermal expansion match. In the MTS technique,[14,15] the substrate is mounted on a platen which is continuously rotated at a programmed frequency through two or more electrically and physically isolated sputtering discharges. Two targets, InSb and GaSb, were used in the present experiments and pseudobinary (In,Ga)Sb films were formed by sequentially depositing partial monolayers of each component. Ion bombardment enhanced diffusion[16,17] during growth was sufficient to allow the formation of homogeneous alloys. X-ray diffraction analysis gave no indication of superlattice compositional modulations.

The MTS system itself has been described in detail previously[15] and will only be discussed briefly here. The system base pressure was ~ 5×10^{-7} Torr (6.7×10^{-5} Pa), achieved in ~ 4 h using a liquid nitrogen trapped 2500 ℓ/sec turbomolecular pump. Sputtering was carried out in 99.998% pure Ar which was further purified by passing it through a Ti sponge getter at 900°C immediately prior to introduction into the vacuum system. The sputtering pressure used was 15 mTorr (2Pa) and the target voltages were varied between 0 and -1500 V depending on the desired composition. The target to substrate separation was 3.9 cm and the substrate rotation rate was 8 rev/min. No

substrate heating was applied. However, the films achieved a steady state growth temperature, T_s, of 100 $\pm$ 20°C due to energetic particle bombardment from the discharges. Film thickness ranged from 0.2 to 4 μm.

Film compositions were determined with a JEOL electron microprobe using single crystal bulk GaSb and InSb wafers as reference standards. Matrix corrections for x-ray fluorescence, absorption, and atomic number were carried out using the Magic IV program.[18] The reported compositions are accurate to better than 0.5 at%. Film structure was analyzed using a Norelco x-ray diffractometer as well as by transmission electron microscopy. In the latter case the films were floated off the substrate in dilute HF. Scanning electron microscopy was used to investigate topographic changes in the films due to ISC. Resistivity and Hall measurements were also made on both pre- and post-transformed samples.

Initiation or triggering of impulse stimulated transformations in amorphous (In,Ga)Sb films required an energy impulse and an ambient sample temperature greater than some critical set of values which depended on the film thermal history and composition. The energy impulse was supplied either mechanically using a stainless steel stylus or optically using a pulsed 0.75 W Ar laser. The stylus had a tip radius of 10 μm and a normal load of 130 g. The stylus velocity upon impact with a film was 10 cm/sec. The Ar laser produced 20 nsec pulses a rate of 10 MHz.

During all experiments the samples were in thermal contact with a heater which had a much larger thermal mass. The temperature of the samples was monitored continuously using a 0.25 mm diameter alumel-chromel thermocouple attached to the top surface of the film. The minimum ambient temperature at which an ISC transformation could be induced, T^*, for a given sample thermal history and composition was determined by heating the sample

from room temperature at a rate of 27°C/min while mechanically impulsing the sample at a frequency of 10 min^{-1}. The transformation was observed by simultaneously monitoring, on an oscilloscope, the electrical resistance across the sample. For this purpose, electrical contacts were made to the edges of the sample using silver ink.

A schematic diagram of the circuit used to determine the onset of ISC is shown in Figure 3. The impacting stylus was used to trigger both the ISC transformation and the oscilloscope sweep. Sample resistance was monitored on strip chart recorder #1 and the film temperature as a function of time was recorded on strip chart recorder #2. When the transformation occurred, a large change in film resistance produced a voltage spike which, through the transformer, was superimposed on the thermocouple output thus delineating T^*.

The rate of film tranformation was determined both by the change in sample resistance and the change in film optical reflectivity with time. A schematic diagram of the apparatus used in the latter technique is shown in Figure 4. A low intensity, 10 mW/cm^2, Ar laser beam expanded into a line 10 mm long by 35 μm wide was focused onto the sample using lens L_2. The reflected light from the sample was in turn focused onto a photodiode by another lens L_1. The photodiode response was then recorded on the oscilloscope which was triggered by the onset of the transformation. The propagation velocity of the transformation was determined from the rate of change of the film reflectivity in the region probed as the crystallization front passed through the parent phase. Experiments, to be described in section III, were carried out to prove that impulse crystallization does not occur simultaneously throughout the film.

III. Experimental Results

Figure 5a and 5b show dark field images and transmission electron diffraction patterns of an $In_{.48}Ga_{.52}Sb$ film before and after complete ISC transformation. The as-deposited film shown in Figure 5a exhibited broad diffraction rings and a small grain (< 100 Å) nearly-amorphous microstructure. After the transformation, the film grain size increased to 500 Å with considerable sharpening of the diffraction rings. Twins, as shown in Figure 5b, could be observed in ISC transformed films.

X-ray diffraction patterns from both an as-deposited and an ISC transformed $In_{.4}Ga_{.6}Sb$ film are shown in Figure 6. The ISC transformation was carried out at $T = T^* \simeq 100°C$ for this alloy.[13] The as-deposited film exhibited no observable structure in the x-ray scan while the transformed film showed a well resolved (111) Bragg peak occurring at the same angular position as found for films of identical composition and grown under the same conditions, only having been post-annealed at 400°C for 2 h. Thus no residual macrostress was observable in the ISC transformed film. Figure 6 also shows an x-ray scan from an $In_{.4}Ga_{.6}Sb$ film which had been annealed at 180°C for 2.5 h. The film was partially crystallized and in this state, ISC could not be induced at any temperature.

The reflectivity of all films decreased after ISC transformation due to surface topographical changes. As-deposited amorphous (In,Ga)Sb films exhibited a smooth featureless surface as observed by scanning electron microscopy (SEM) at magnifications of up to 5000 x. Figure 7a shows an SEM micrograph of a GaSb film transformed at a temperature $T^* \simeq 90°C$. The transformed surface exhibits regular undulations radiating from the triggering point. A similar surface morphology was obtained from an identical GaSb sample grown in the same deposition but which pre-annealed for 1 h at 175°C. The thermal treatment increased T^* to 180°C.

In all ISC-transformed films investigated, the surface structure appeared to have radiated from the triggering point. A further indication of this type of behavior is shown in Figure 8, a low magnification bright field transmission electron micrograph of a GaSb film transformed at a temperature $\simeq T^*$. The contrast is due to density fluctuations in the film caused by incomplete crystallization within each domain. The fluctuations are periodic with a wave vector given by the arrow which is pointing radially away from the triggering point signifiying a cascade process proceeding from domain to domain.

The regularity of the surface structure in transformed films may be increased by carrying out the transformation at temperatures greater than T^*. This is indicated by a comparison of Figures 9a and 9b which show SEM micrographs of $In_{.35}Ga_{.65}Sb$ films of the same thickness transformed at 100°C ($\sim T^*$) and 220°C, respectively. Carrying out the transformation at temperatures much greater than T^* allows the entire domain to completely crystallize eliminating the periodic undulations due to changes in density between completely and pa r tially crystallized regions within each domain.

The increase in T^* with increasing mole % InSb in the film (e.g., 90°C for GaSb to 100°C for $In_{.35}Ga_{.65}Sb$) has been reported previously and is dut to the increase in the crystallinity of the as-deposited film. Figure 10 shows x-ray diffraction scans of as-deposited alloy films of different compositions. The diffraction patterns from films with less than $\sim$ 50 mole % InSb exhibited no sharp peaks at all, while a (220) Bragg reflection, clearly shown for the $In_{.60}Ga_{.40}Sb$ sample, began to appear in patterns taken from samples with greater than 50 mole % InSb. Polycrystalline III-V films deposited on glass substrates typically exhibit a strong (110) preferred orientation.[17]

An experiment was designed to prove that the crystallization front does in fact propagate radially from the triggering point rather than the entire film crystallizing simultaneously. A low energy laser beam was expanded into a line as described in section II. The beam was then oriented to illuminate a stripe along either the x or y-axis of the film as shown in Figure 11 by rotating lens L_2 (see Figure 4). In case I the irradiated line was along a radial direction from the triggering point and in case II the irradiated line was perpendicular to the radial direction. The change in reflectivity of the irradiated region of the film was then determined as a function of time after ISC triggering using the apparatus described in section II. If the transformation occurred simultaneously throughout the film, the time derivative of the detected signal would be approximately the same in both cases. However, if the crystallization front propagated radially outward from the triggering point, then the results from the case I experiments would exhibit a much smaller time derivative than in case II as shown schmatically in Figure 11. The results, shown in Figure 12 for a GaSb film, indicated that the crystallization front indeed propagates radially. An analysis of the results yielded a propagation velocity, v, of ~ 300 cm/sec.

The rate of increase in the sample current for a given applied voltage during ISC was also used to estimate the propagation velocity. A typical result for a GaSb film transformed at T^* is shown in Figure 13. The contact spacing was 0.5 cm yielding a propagation velocity of 330 cm/sec. In general, v was found to vary between 100 and 400 cm/sec depending on film composition and thermal history.

All amorphous $In_{1-x}Ga_xSb$ films could be made to exhibit an ISC transformation locally near the point of impulse. Whether or not the transformation propagated throughout the film was found to depend on the thermal

history of the sample and the temperature at which the experiment was carried out, as has been shown, as well as on the film thickness. A set of samples of different compositions were grown with gradients in film thickness. In no case could ISC propagation be initiated in films thinner than 1.5 μm. If the phase transformation was initiated in a thick region, its propagation was halted abruptly at regions of the sample where the thickness was less than 1.5 μm. Propagation of the transformation was also suppressed in regions of the film which had been covered with thick overcoatings of In_2O_3 or silver ink. However, propagation continued for overlayers with thicknesses less than 1000 Å.

IV. Thermal Transport Model of ISC

ISC can be described and analyzed using a simple thermal transport model. The as-deposited films are in a metastable state A as shown schematically in Figure 14 and require an activation energy, E_a, to transform them into a stable state B. E_a is a material constant and in the case of (In,Ga)Sb, E_a was found to decrease with increasing InSb content. The enthalpy of crystallization per unit volume, ΔH_c, shown schematically in Figure 14, is also a material property. The total heat released per unit volume during an exothermic ISC process is given by

$$Q_c = \Delta\xi \cdot \Delta H_c \qquad (1)$$

where $\Delta\xi$ is the fractional volume of film in metastable state A.

An amorphous film may be crystallized by heating it to a sufficiently high temperature to allow grain growth from nucleation sites distributed throughout the entire film. Alternately, crystallization can occur exteremely rapidly ($< 10^{-5}$ sec) in a local region or domain of the film which has been subjected to an energy impulse of sufficient magnitude to

provide E_a. The heat released from crystallization of this domain, $q_c = Q_c V_d$, where V_d is the domain volume, is then dissipated by conduction throughout the film as well as by heat loss to the substrate, q_s. Radition losses from the film surface can generally be neglected. If the heat transferred from the impulse crystallized domain to the adjacent incipient domain, q_d, is sufficient, then it will also crystallize and the process can cascade throughout the film. Depending on the values of E_a, ΔH_c, q_s, and the thermal conductivity of the film k_f, additional external heating of the sample may also have to be supplied in order to achieve propagation of ISC. For example, comparing Ge and GaSb, ΔH_c is large enough with respect to E_a that propagation of ISC occurs at room temperature in Ge, but GaSb must be heated to $\gtrsim$ 90°C in order to propagate the crystallized region.

We have shown in section III that the ISC crystallization front emanates radially from the triggering point as shown schematically in Figure 15. In our analysis we will then consider a segment of the film which has a length δ of unity, a width λ, and thickness h. We assume that at time t = 0, the temperature of the film segment is T_1 due to external heating as well as to the heat released from the crystallization of inner domains. However, T_1 is still less than T_{min}, the minimum domain temperature at which ISC occurs. At the instant, t = 0, the inner domain adjacent to the film segment of interest releases q_c which raises the temperature of the segment. If the temperature of the film segment is increased such that it is everywhere greater than T_{min} for a time $t > \tau_i$, where τ_i is the time required for crystallization, then the film segment itself will crystallize.

Crystallization of the film segment shown in Figure 15 requires that

$$q_d > q_{min} \tag{2}$$

during τ_i where

$$q_{min} = C_f (T_{min} - T_1) V_d \tag{3}$$

and C_f is the heat capacity per unit volume of the as-deposited film. At any given time t following crystallization of the adjacent domain, the portion of q_c released from this domain which still remains in the film is given by q_f and

$$q_d = \gamma q_f = \gamma(q_c - q_s) \tag{4}$$

where γ is the fraction of q_f transferred to the film segment. γ depends upon the product $k_f h$, and, to a lesser extent, upon the ratio of the thermal conductivities of the as-deposited and crystallized regions.

The equation governing the amount of heat lost to the substrate due to crystallization of a domain is of the same general form as the equation derived for the heat lost from a small local region of the film irradiated by a single laser pulse.[19,20] The boundary conditions in the present case are considerably more complicated since we can not assume that the temperature is homogeneous throughout the domain and that the domain length is small with respect to the film thickness as is done in pulsed laser heating. Thus closed form solutions cannot be obtained. Nevertheless, the functionality of the general solution is the same and given by

$$q_s = q_c \, f(\varphi) \tag{5}$$

where $f(\varphi)$ is a positive function of the reduced time variable φ which is give given by

$$\varphi = \frac{C_s k_s \tau_i}{C_f^2 h^2} \tag{6}$$

In the above equation, C_s and k_s are the heat capacity and thermal conductivity, respectively, of the substrate. Independent of the boundary conditions chosen, $f(\varphi)$ must be a continuous function whose value approaches zero when φ approaches zero and approaches unity when φ approaches infinity. Combining equations (2), (4), and (5) gives

$$q_{min} < \gamma q_c [1 - f(\varphi)]. \tag{7}$$

Substituting the definitions of q_c and φ into equation (7), we finally obtain a functional expression of the requirement for impulse crystallization to propagate:

$$q_{min} < \gamma V_d(\Delta\xi)(\Delta H_c)\left[1 - f\left(\frac{C_s k_s \tau_i}{C_f^2 h^2}\right)\right] \tag{8}$$

V. Discussion

It is possible using vapor phase deposition techniques such as evaporation and sputtering to obtain sufficiently rapid thermal quenching rates to deposit metastable amorphous films.[21] In such metastable films there is an activation barrier, E_a, necessary to transform the material into the equilibrium crystalline state. This activation energy, typically 40 to 100 meV, is often expressed as the annealing temperature, T_a, at which normal crystallization occurs in 1 h. For example, $T_a \simeq 450°C$ for evaporated amorphous Ge and $\simeq 240°C$ for sputtered amorphous GaSb.

Chopra[22] investigated amorphous to crystalline transformations in Ge films occurring due to normal nucleation and grain growth and found that the total time required for complete film crystallization could be described by

$$\tau_i = \tau_o \exp(E_a/kT) \tag{9}$$

where τ_o and E_a both varied with film purity and growth conditions. The addition of various metallic impurities, at concentrations of up to 5 at %, resulted in τ_o values ranging from 3.2×10^{-29} sec to 5×10^{-18} sec while E_a varied from 3.1 eV to 1.5 eV. Kennedy et al.[23] found that the presence of oxygen, carbon, nitrogen, and noble gases in amorphous Si tended to impede crystallization by increasing E_a. Film stress can also significantly alter the free energy of the film and affect the activation energy of crystallization.[24] E_a for InSb films sputter deposited onto 7059 glass substrates under the same

conditions as the GaSb films reported here, is sufficiently small that the films are crystalline as-deposited at ambient temperatures, ~ 100°C. For $In_{1-x}Ga_xSb$ alloys, E_a increases with increasing mole % GaSb until, for films with greater than 40 mole % GaSb, no Bragg peaks are observed in x-ray diffraction patterns.

Impulse stimulated crystallization is a process in which an amorphous film is crystallized in a cascading manner, domain by domain, rather than by random nucleation and growth occurring throughout the film. In ISC, only a limited region of the film is pulsed with sufficiently high energy for a time period τ_i to allow crystallization. The heat of crystallization released by this exothermic reaction provides the "energy pulse" for the next domain to crystallize, etc. In principle, a local region of an amorphous film can always be crystallized by providing a large enough energy pulse over a sufficiently short time to minimize thermal loss. Whether or not, the crystallization process will cascade throughout the film depends on film growth conditions through parameters such as $\Delta\xi$ and h, material parameters such as E_a and ΔH_c, and experimental conditions such as the temperature and the volume of the initial domain. The critical functional relationship between these various parameters is expressed in equation (8).

The value of T_{min}, the critical temperature of the domain as it undergoes ISC, can be estimated for Ge from reported values of the domain size and the total time required to crystallize the film combined with Chopra's measurements of τ_o and E_a for pure Ge. Thus, for a value of $\tau_i = 10^{-6}$sec, corresponding to a propagation velocity of ~ 100 cm/sec for a domain length of 10^{-4}cm, $T_{min} \simeq 860$°C. While this temperature is larger than reported measurements, typically ~ 500°C,[8,9] the experiments were carried out such that the measured temperature was either an average over a very large spatial

region of which only one domain was crystallizing at a time (infrared pyrometry[8]) or an average over a long time period with respect to a given impulse crystallization event (differential thermal analysis[9]). There is also some experimental evidence that T_{min} may be much larger than 500°C. Triboluminescence ranging in wavelength from the infrared down into the visible spectrum has been observed during ISC of Ge.[10] The emission of visible light in Ge only begins to occur at a surface temperature of > 700°C.

The effects of sample heating or cooling on ISC can be explained using equations (3) and (8). Decreasing the initial sample temperature T^* (hence T_1 in equation (3)), increases q_{min} and below some critical temperature the inequality given by equation (8), which expresses the necessary condition for ISC propagation, will not hold. This explains the observation reported by Matsuda et al.[8] that ISC propagation in Ge, which can be actuated at room temperature, is suppressed by cooling the sample to 77°K. Similarly, in the case of $In_{1-x}Ga_xSb$ films, T^* was found to increase with increasing mole % InSb due to a concomitant decrease in both $\Delta\xi$, the volume fraction of amorphous material, and ΔH_c, the enthalpy of crystallization. A decrease in either of these terms decreases the right side of the inequality in equation (8). The volume fraction of amorphous material can also be decreased by annealing the film prior to ISC transformation and allowing the film to partially crystallize by normal processes. Such a pre-anneal will thus increase T^* and at some point prevent ISC propagation from occurring at all.

The film thickness effect in ISC transformations can also be explained using equation (8). A decrease in the film thickness, h, reduces the value of the right side of the inequality and at some point the equation predicts that

ISC will no longer propagate as is observed experimentally. The critical value of h is determined by thermal losses from the film. That is, as h decreases, $f(\varphi)$ approaches unity and q_s approaches q_c. Finally, equation (8) predicts that ISC will be more difficult to propagate as the heat capacity and the thermal conductivity of the substrate increase. Encapsulation of the film has the effect of increasing the thermal loss from the film and for all other conditions held constant, ISC propagation will be halted at a critical encapsulation layer thickness which depends on the thermal constants of the layer.

A practical application of ISC in materials like $In_{1-x}Ga_xSb$, for which T^* is greater than room temperature, is information storage. Pulsed lasers can be used to "write" on the film producing either positive or negative images. In order to produce a positive image, the film is maintained at a temperature less than T^* and subjected to a series of laser pulses. The first few pulses heat the irradiated region to a temperature greater than T^*, while the next pulse transforms a single domain. Propagation does not occur throughout the film since $T < T^*$. The information may be "read" by rastering a low energy laser beam, such as from a He-Ne laser, across the transformed region and monitoring the change in reflectivity with a photodiode. The reflectivity of the transformed region is significantly less than that from the matrix.

A negative image may be produced by adjusting the power output of a laser beam to anneal a local region of the film, a spot or a line for example, initiate normal crystallization, and raise T^* in this region. The entire film is then heated above the initial T^*, and ISC propagation induced using a higher energy laser pulse. The pre-annealed regions will not transform

by ISC and thus their reflectivity will remain high while that of the transformed matrix will be significantly lower.

Spot or line resolutions on the order of 1 μm may be obtained using the negative image technique. It appears that this resolution is limited both by focusing optics of the laser beam itself and by the minimum obtainable undulation period. A considerable increase in resolution may be possible using electron beam writing to produce a positive image. In this case, contrast during reading might be provided by monitoring the sample current to ground if the resistivity ratio is sufficiently large or by monitoring changes in secondary electron yields.

Acknowledgements

The authors gratefully acknowledge the financial support of the Joint Services Electronics Program (U.S. Army, U.S. Navy, and U.S. Air Force) under Contract DAAB-07-72-C-0259 and the International Research Exchange Board during the course of this work.

References

1. D. Adler, "Amorphous Semiconductors," CRC Press, Cleveland (1971).

2. "International Conf. on Tetrahedrally Bonded Amorphous Semiconductors," Yorktown Heights, New York, edited by M. H. Brodsky, S. Kirkpatrick, and D. Weaire, American Inst. Physics, New York (1974).

3. J. Feinleib, J. DeNeufville, S. C. Moss, and S. R. Ovsinsky, Appl. Phys. Letters 18, 254 (1971).

4. G. Gore, Phil. Mag., 9, 73 (1955)

5. F. M. Americh and A. Delunas, Phys. Stat. Sol (A) 31, 165 (1975).

6. T. Takamori, R. Messier, and R. Roy, Appl. Phys. Lett., 20, 201 (1972).

7. A. Mineo, A. Matsuda, T. Kurosu, and M. Kikuchi, Solid State Commun. 13, 329 (1973).

8. A. Matsuda, A. Mineo, T. Kurosu, and M. Kikuchi, Solid State Commun. 13, 1165 (1973).

9. T. Takamori, R. Messier, and R. Roy, J. Mat. Sci. 8, 1809 (1973).

10. T. Takamori, R. Messier, and R. Roy, J. Mat. Sci. 9, 159 (1974).

11. M. Kikuchi, A. Matsuda, T. Kurosu, A. Mineo, and K. J. Callan, Solid State Commun. 14, 731 (1974).

12. V. I. Zaliva, V. P. Zakharov, and Y. M. Polskii, Neorganicheskie Materialy 7, 1702 (1971).

13. C. E. Wickersham, G. Bajor, and J. E. Greene, Solid State Commun. 27, 17 (1978).

14. C. E. Wickersham and J. E. Greene, J. Appl. Phys. 47, 4734 (1976).

15. J. E. Greene, C. E. Wickersham, and J. L. Zilko, J. Appl. Phys. 47, 2289 (1976).

16. A. H. Eltoukhy and J. E. Greene, Appl. Phys. Letters 33, 343 (1978).

17. A. H. Eltoukhy and J. E. Greene, J. Appl. Phys. 50, 505 (1979).

18. J. W. Colby, Materials Research Laboratory, University of Illinois, Urbana (unpublished).

19. R. A. Ghez, and R. A. Laff, J. Appl. Phys. 46, 2103 (1975).

20. U. C. Paek and A. Kestenbaum. J. Appl. Phys. 44, 2260 (1973).

21. See, for example, the review article by A. K. Sinha, B. C. Giessen, and D. E. Polk, in "Treatise on Solid State Chemistry, Vol. 3," edited by N. B. Hannay, Plenum Press, New York (1976).

22. K. L. Chopra, H. S. Randhawa, and L. K. Malhotra, Thin Solid Films 47, 203 (1977).

23. E. F. Kennedy, L. Csepregi, J. W. Mayer, and T. W. Sigmon, J. Appl. Phys. 48, 4241 (1977).

24. G. A. Walker, V. C. Marcotte, and R. M. Anderson, Thin Solid Films 33, 43 (1976).

Figure Captions

1. Resistance across the sample vs measurement temperature for amorphous GaSb films heat at a rate of 27°C/min. (A) As-deposited film, (B) Film pre-annealed at 180°C for 90 min. (C) An as-deposited GaSb film crystallized by normal nucleation and grain growth.
2. Minimum ISC transition temperature for $In_{0.4}Ga_{0.6}Sb$ films as a function of pre-annealing time at 135 and 175°C.
3. Schematic diagram of the circuit used to determine the onset of ISC.
4. Schematic diagram of the apparatus used for optically probing the ISC transformation. The beam geometry in case I and case II is shown in Figure 11.
5. Transmission electron microscopy dark field images and electron diffraction patterns from an $In_{0.48}Ga_{0.52}Sb$ film (A) before and (B) after ISC transformation.
6. X-ray diffraction patterns from $In_{0.4}Ga_{0.6}Sb$ films in the as-deposited state, after annealing for 2.5 h at 180°C, and after ISC transformation at 100°C.
7. A scanning electron micrograph showing the surface topography of an ISC transformed GaSb film.
8. Bright field transmission electron micrograph of an ISC transformed GaSb film. The arrow indicates the direction of propagation of the crystallization front.
9. Scanning electron micrographs of ISC transformed $In_{0.35}Ga_{0.65}Sb$ films in which the transformation was carried out at (A) $T^* = 100$°C and (B) 220°C.
10. X-ray diffraction scans of as-deposited $In_{1-x}Ga_xSb$ films grown at ambient temperature on Corning 7059 glass substrates.

11. Schematic diagrams of optical probing experiments for investigating impulse stimulated crystallization.

12. Results of optical probing experiments investigating impulse stimulated crystallization of an amorphous GaSb film. Case I and case II refer to the laser beam geometries shown in Figure 11.

13. The change in the current flowing through the sample in response to a constant applied voltage during impulse stimulated crystallization of a GaSb film.

14. Schematic diagram showing the energy levels of the metastable and crystalline states of GaSb and $In_{0.25}Ga_{0.75}Sb$ films, respectively. E_a is the activation energy for crystallization of an amorphous film and ΔH_c is the enthalpy of crystallization.

15. Schematic diagram indicating a segment of a ring shaped domain during the propagation of an impulse stimulated crystallization front.

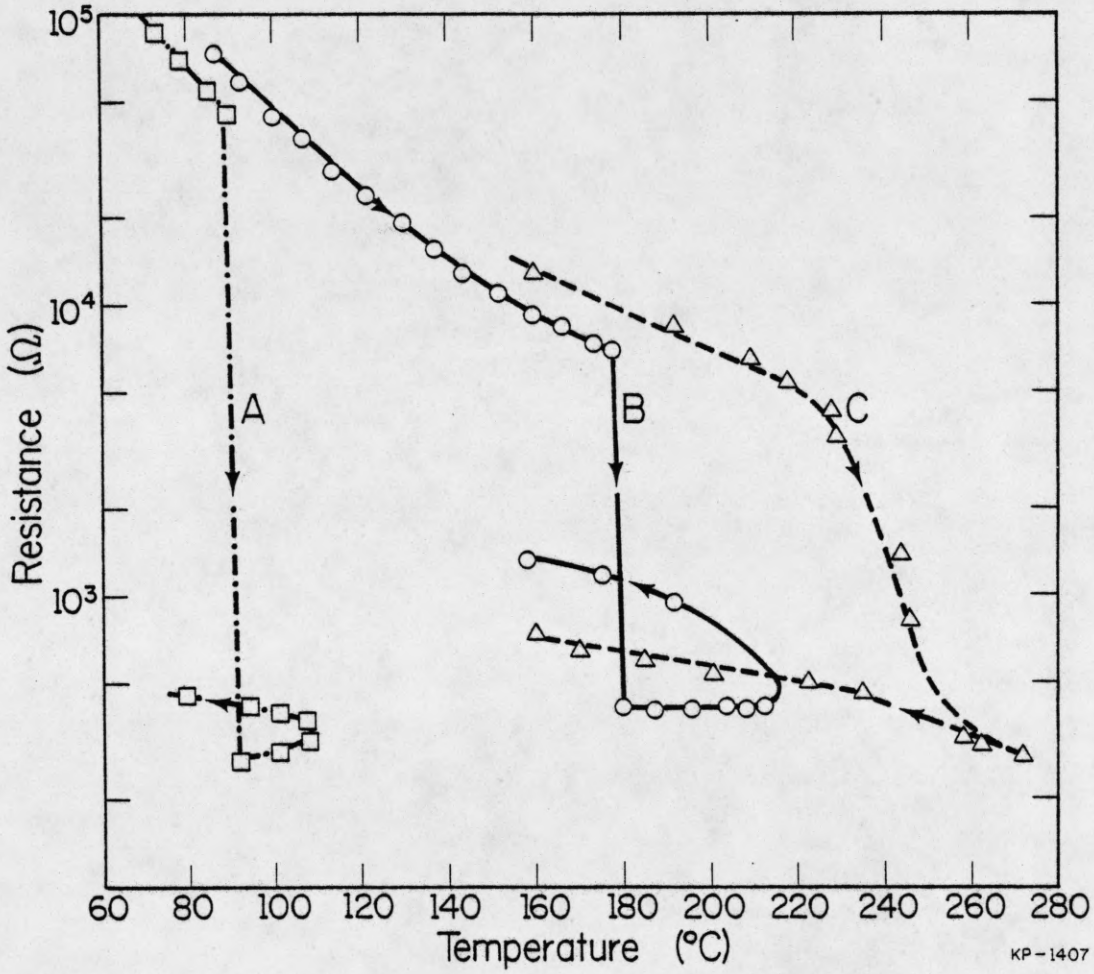

1. Resistance across the sample vs measurement temperature for amorphous GaSb films heat at a rate of 27°C/min. (A) As-deposited film, (B) Film pre-annealed at 180°C for 90 min. (C) An as-deposited GaSb film crystallized by normal nucleation and grain growth.

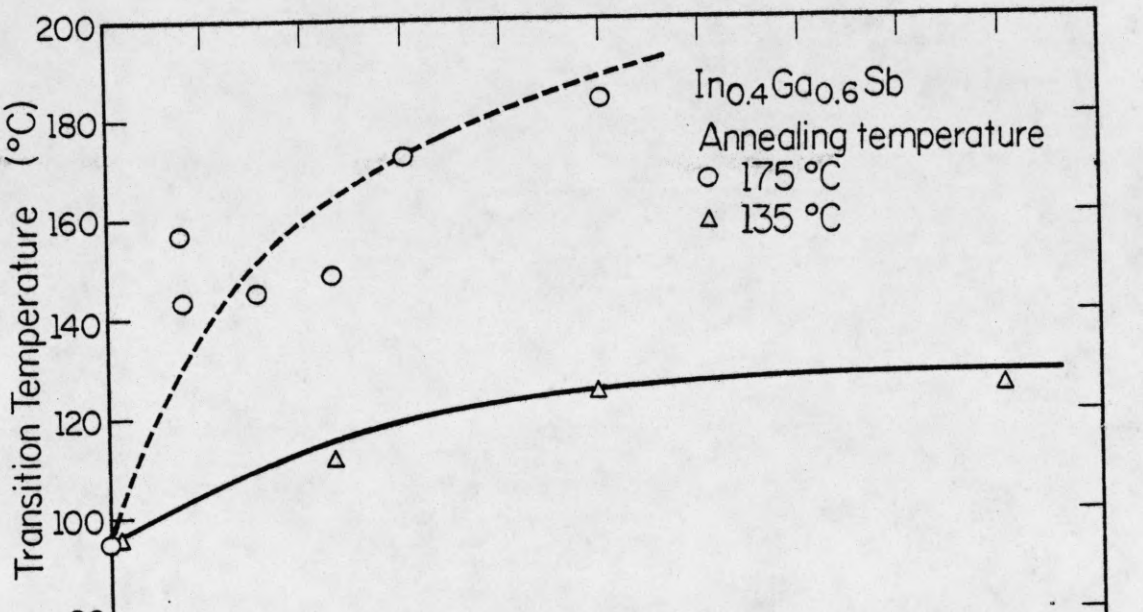

2. Minimum ISC transition temperature for $In_{0.4}Ga_{0.6}Sb$ films as a function of pre-annealing time at 135 and 175°C.

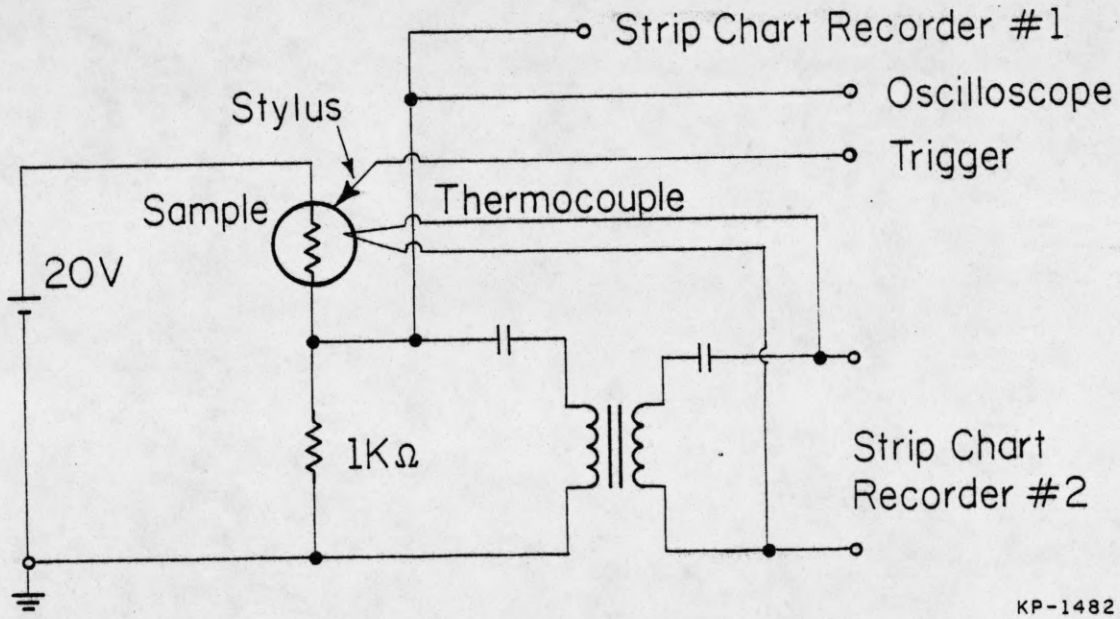

3. Schematic diagram of the circuit used to determine the onset of ISC.

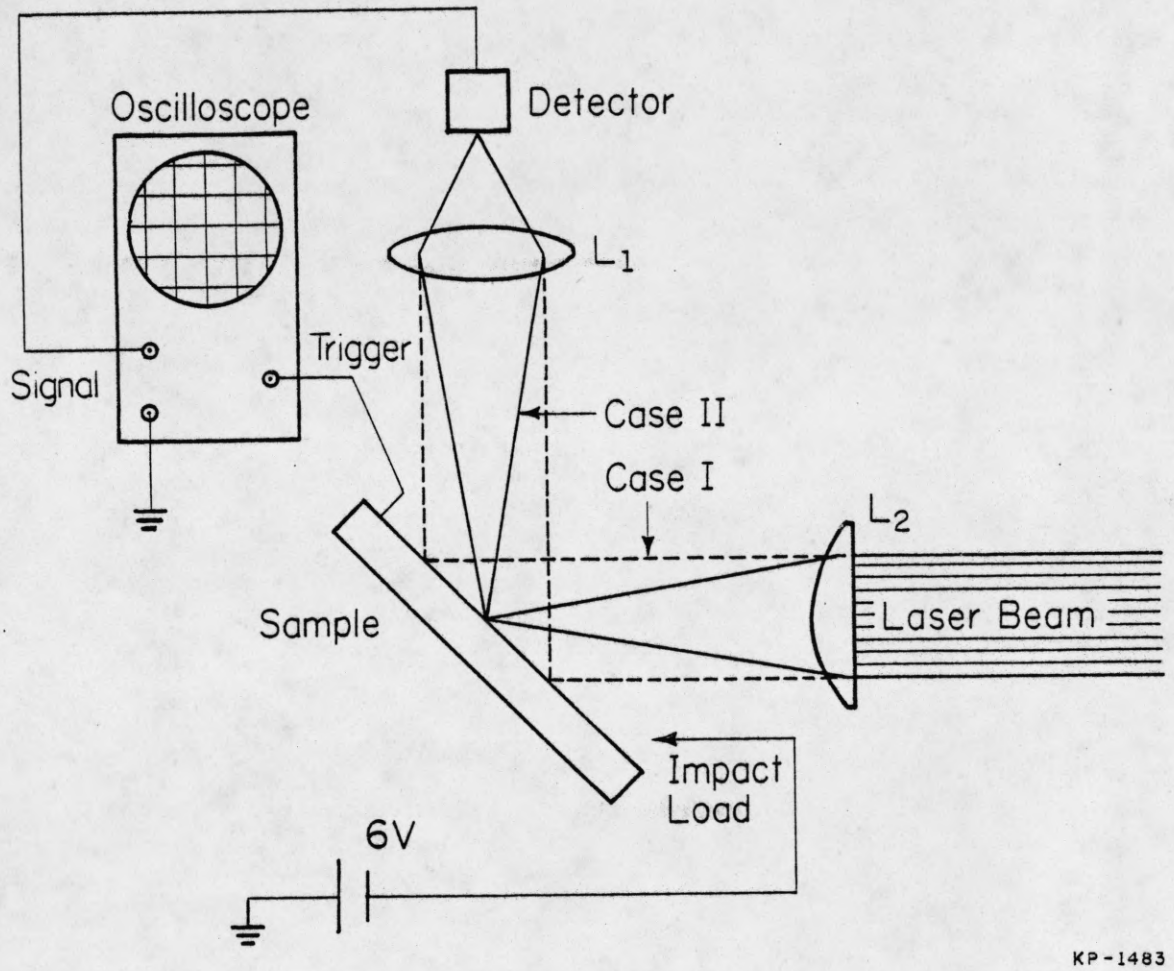

4. Schematic diagram of the apparatus used for optically probing the ISC transformation. The beam geometry in case I and case II is shown in Figure 11.

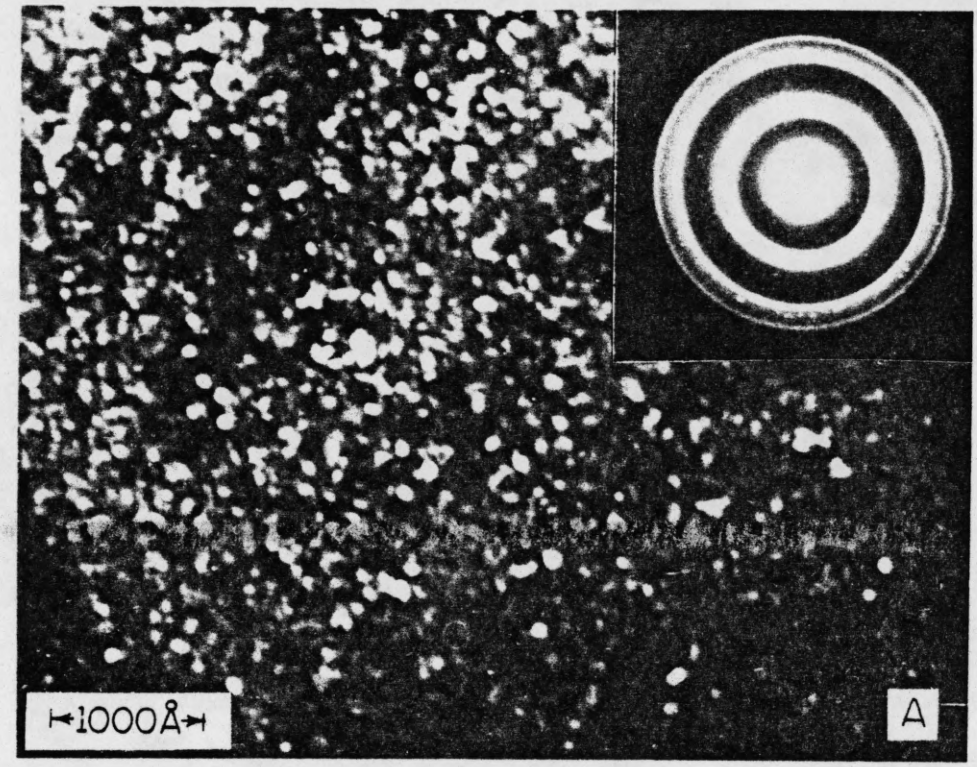

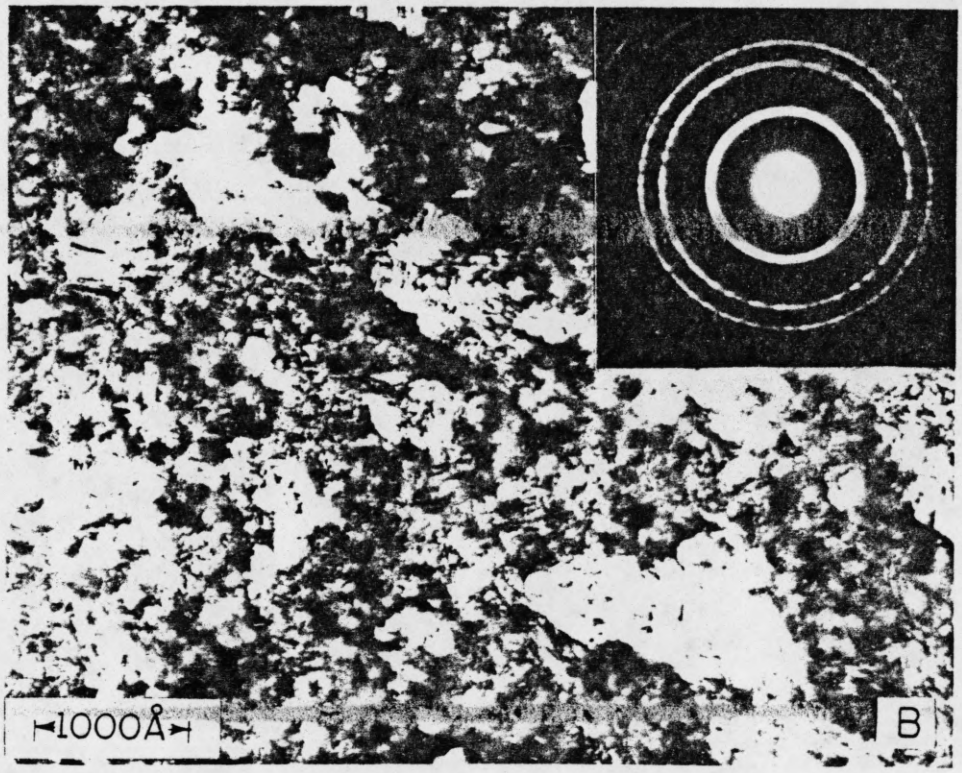

5. Transmission electron microscopy dark field images and electron diffraction patterns from an $In_{0.48}Ga_{0.52}Sb$ film (A) before and (B) after ISC transformation.

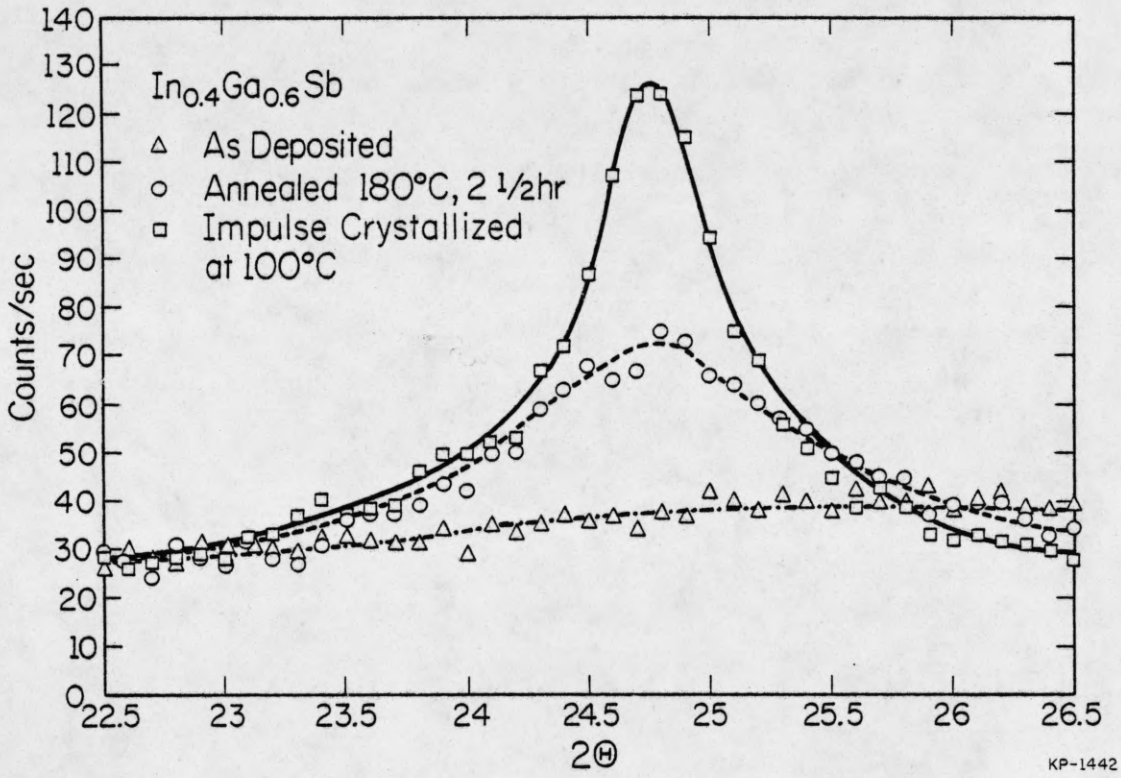

6. X-ray diffraction patterns from $In_{0.4}Ga_{0.6}Sb$ films in the as-deposited state, after annealing for 2.5 h at 180°C, and after ISC transformation at 100°C.

7. A scanning electron micrograph showing the surface topography of an ISC transformed GaSb film.

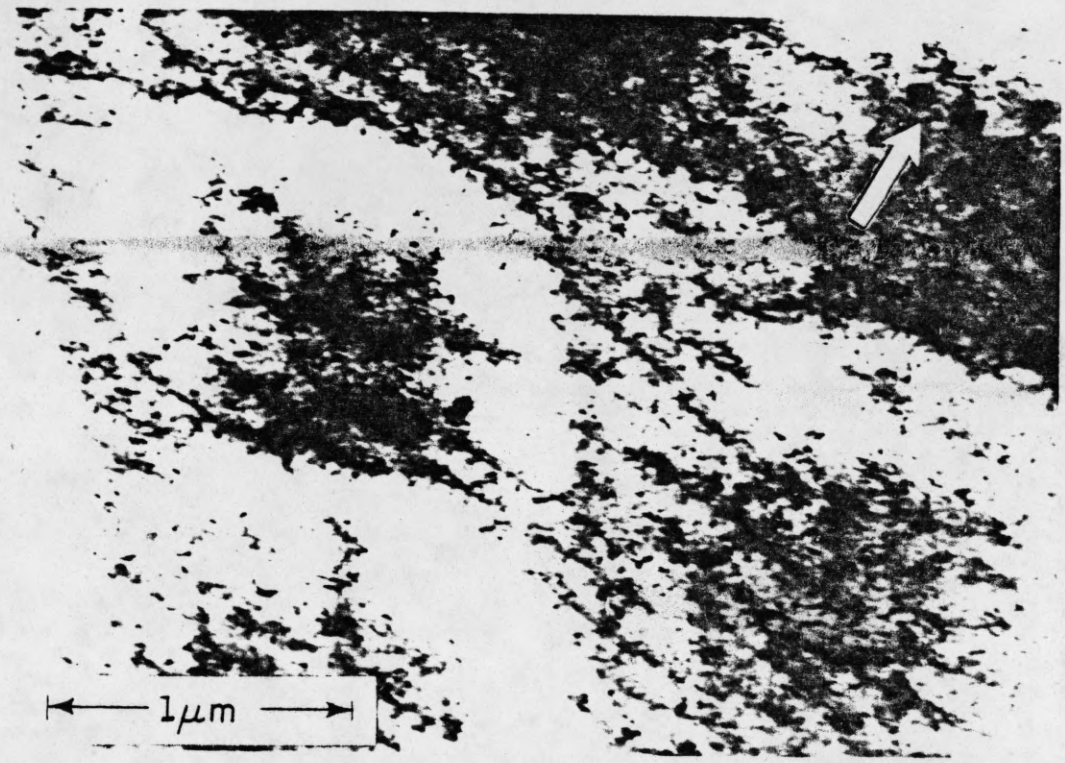

8. Bright field transmission electron micrograph of an ISC transformed GaSb film. The arrow indicates the direction of propagation of the crystallization front.

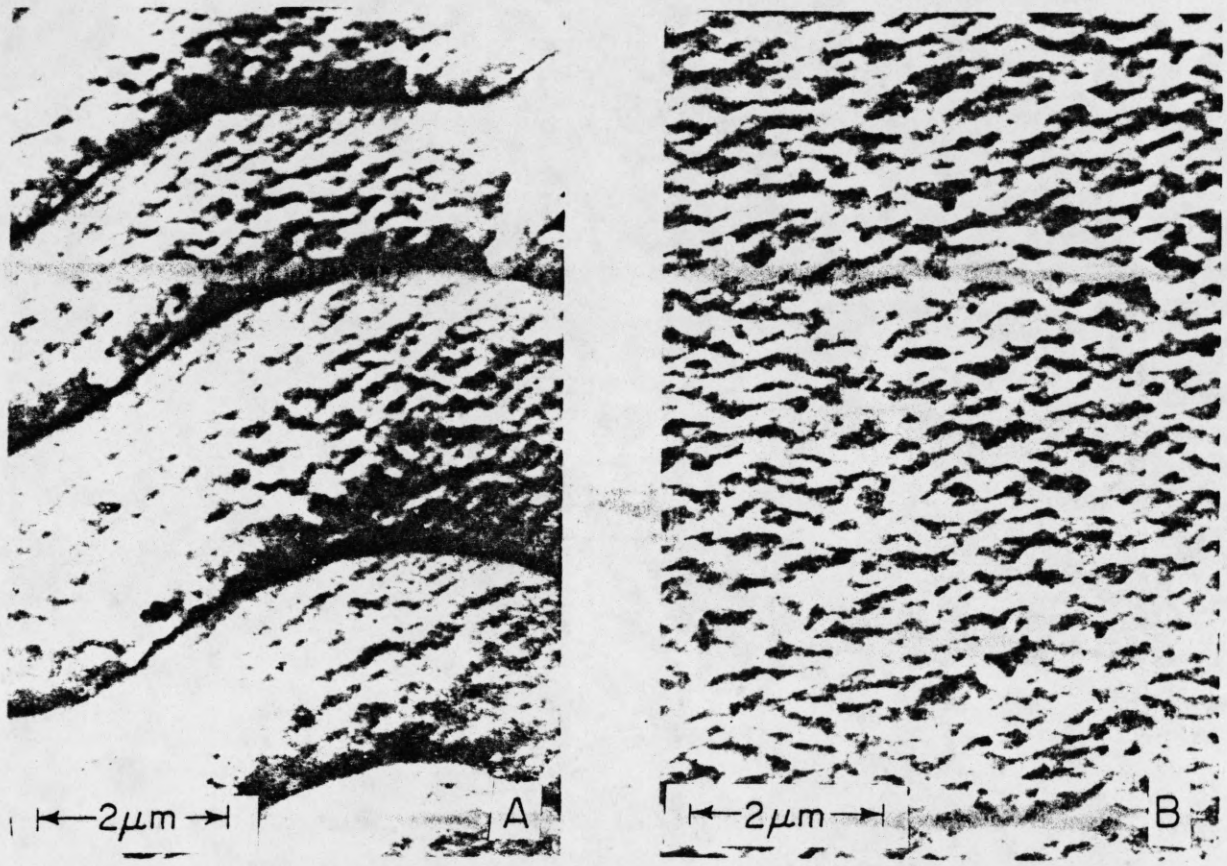

9. Scanning electron micrographs of ISC transformed $In_{0.35}Ga_{0.65}Sb$ films in which the transformation was carried out at (A) T^{*} = 100°C and (B) 220°C.

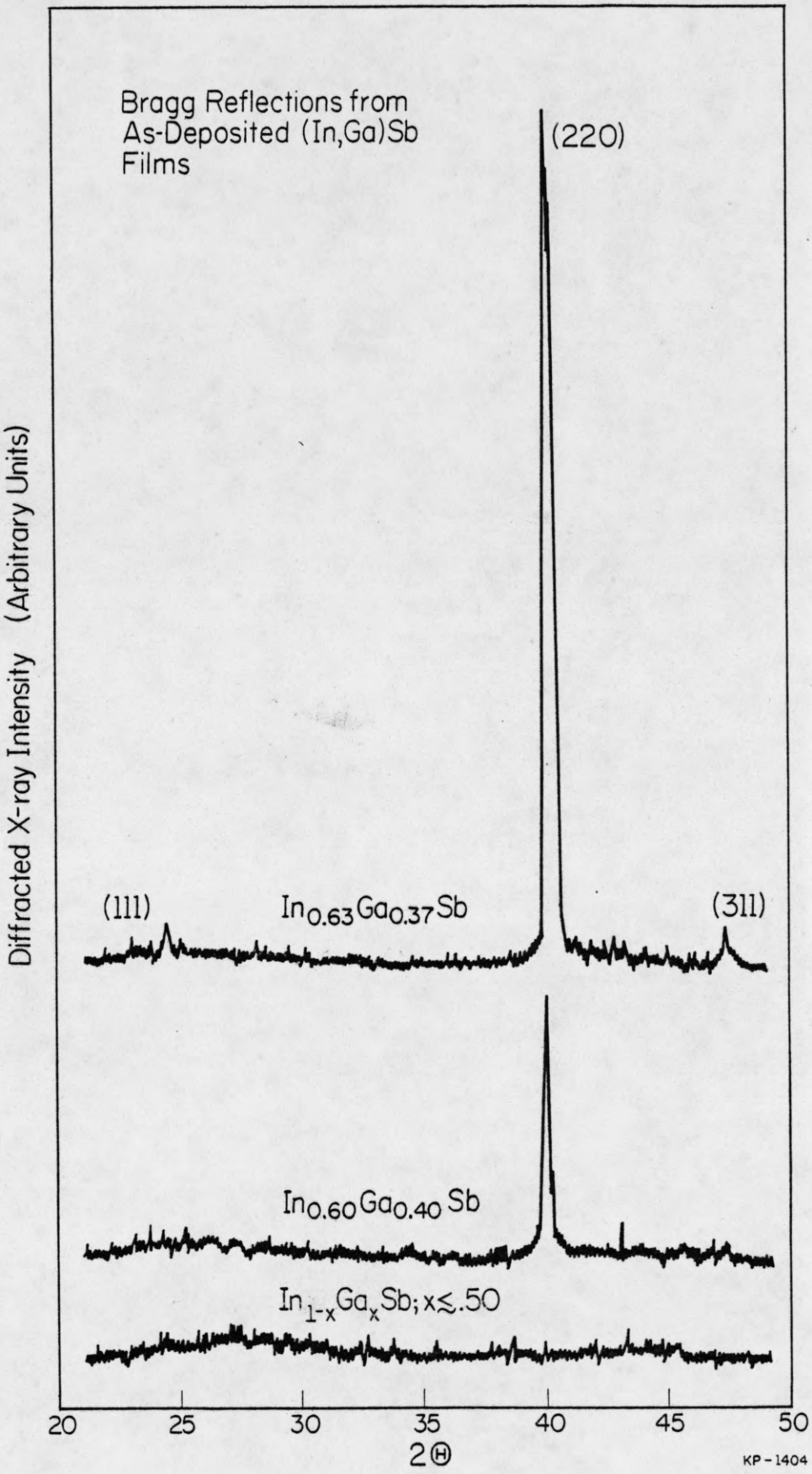

10. X-ray diffraction scans of as-deposited $In_{1-x}G_{ax}Sb$ films grown at ambient temperature on Corning 7059 glass substrates.

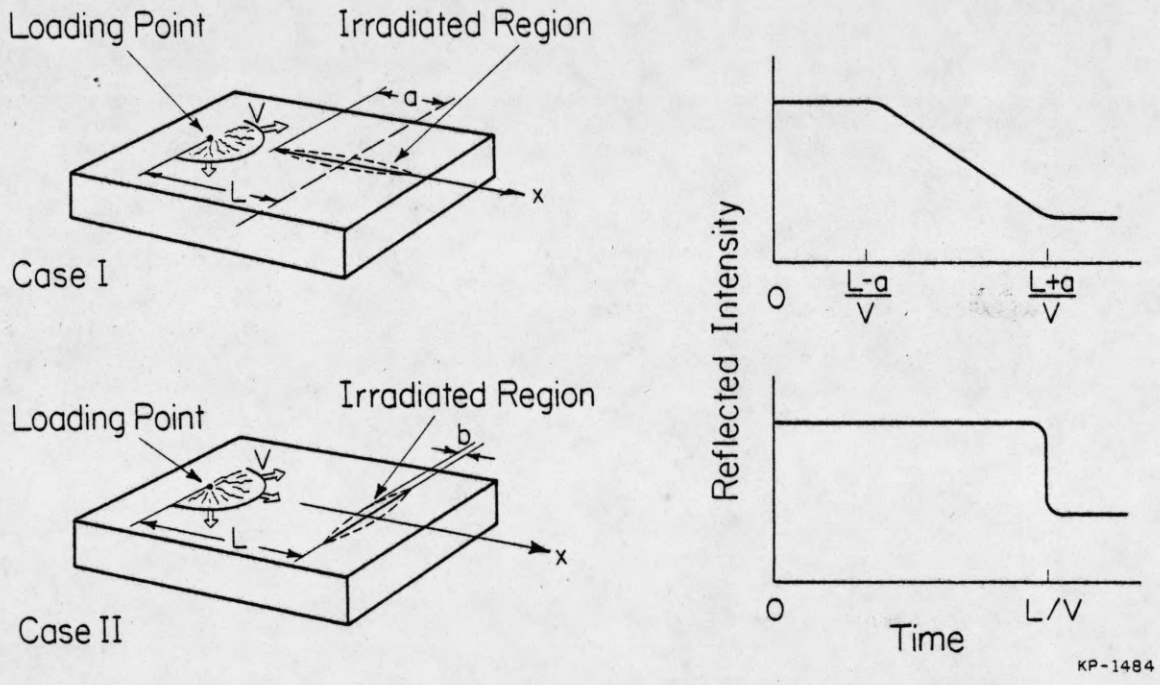

11. Schematic diagrams of optical probing experiments for investigating impulse stimulated crystallization.

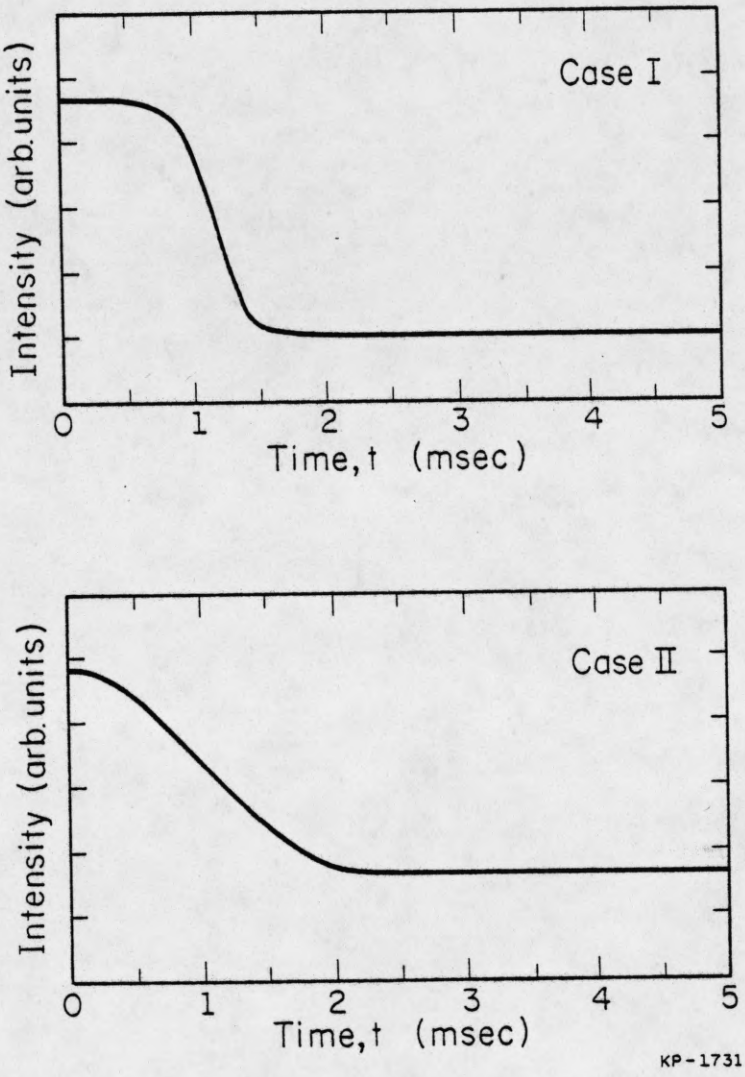

12. Results of optical probing experiments investigating impulse stimulated crystallization of an amorphous GaSb film. Case I and case II refer to the laser beam geometries shown in Figure 11.

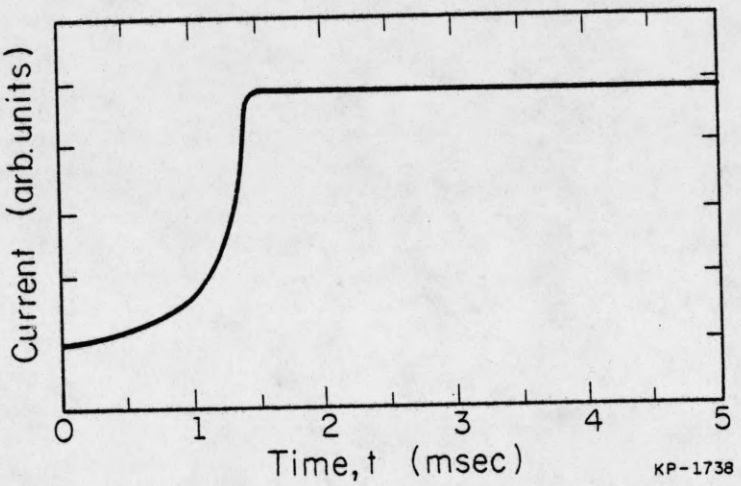

13. The change in the current flowing through the sample in response to a constant applied voltage during impulse stimulated crystallization of a GaSb film.

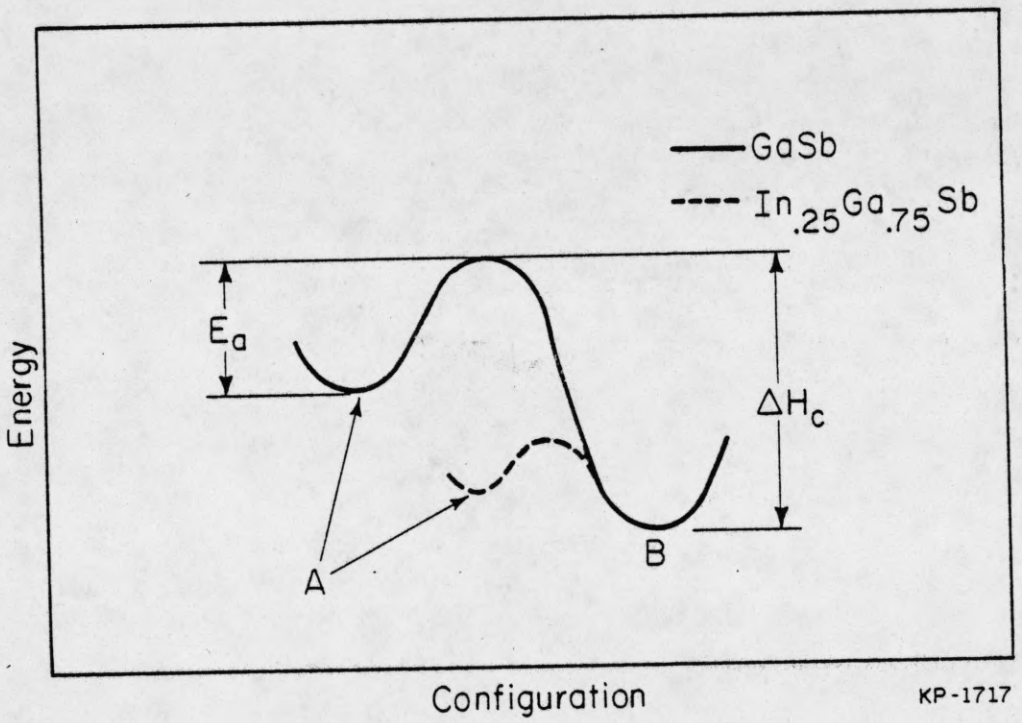

14. Schematic diagram showing the energy levels of the metastable and crystalline states of GaSb and $In_{0.25}Ga_{0.75}Sb$ films, respectively. E_a is the activation energy for crystallization of an amorphous film and ΔH_c is the enthalpy of crystallization.

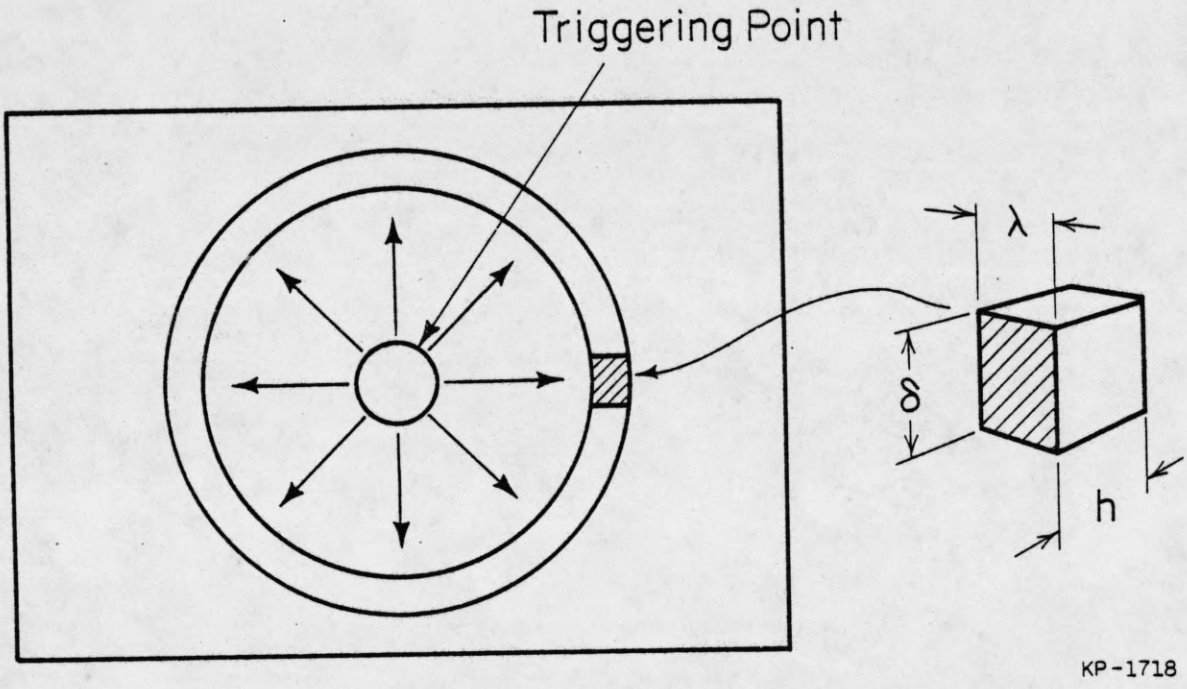

15. Schematic diagram indicating a segment of a ring shaped domain during the propagation of an impulse stimulated crystallization front.